Received: 5 May 2023 | Accepted: 19 October 2023

DOI: 10.1097/HC9.0000000000000338

ORIGINAL ARTICLE

OPEN

FAT4 loss initiates hepatocarcinogenesis through the switching of canonical to noncanonical WNT signaling pathways

Fung-Yu Huang[1] | **Danny Ka-Ho Wong**[1,2] | **Lung-Yi Mak**[1,2] | **Tan-To Cheung**[2,3] | **Sai-Sai Zhang**[1] | **Hau-Tak Chau**[1] | **Rex Wan-Hin Hui**[1] | **Wai-Kay Seto**[1,2] | **Man-Fung Yuen**[1,2]

[1]Department of Medicine, School of Clinical Medicine, The University of Hong Kong, Queen Mary Hospital, Hong Kong SAR

[2]State Key Laboratory of Liver Research, The University of Hong Kong, Hong Kong SAR

[3]Department of Surgery, School of Clinical Medicine, The University of Hong Kong, Queen Mary Hospital, Hong Kong SAR

Correspondence
Man-Fung Yuen, Department of Medicine, The University of Hong Kong, Queen Mary Hospital, Pokfulam Road, Hong Kong.
Email: mfyuen@hku.hk

Wai-Kay Seto, Department of Medicine, The University of Hong Kong, Queen Mary Hospital, Pokfulam Road, Hong Kong.
Email: wkseto@hku.hk

Abstract

Background: Mutation and downregulation of FAT atypical cadherin 4 (FAT4) are frequently detected in HCC, suggesting a tumor suppressor role of FAT4. However, the underlying molecular mechanism remains elusive.

Methods: CRISPR-Cas9 system was used to knockout FAT4 (*FAT4*-KO) in a normal human hepatic cell line L02 to investigate the impact of FAT4 loss on the development of HCC. RNA-sequencing and xenograft mouse model were used to study gene expression and tumorigenesis, respectively. The mechanistic basis of FAT4 loss on hepatocarcinogenesis was elucidated using *in vitro* experiments.

Results: We found that *FAT4*-KO disrupted cell-cell adhesion, induced epithelial-mesenchymal transition, and increased expression of extracellular matrix components. *FAT4*-KO is sufficient for tumor initiation in a xenograft mouse model. RNA-sequencing of *FAT4*-KO cells identified PAK6-mediated WNT/β-catenin signaling to promote tumor growth. Suppression of PAK6 led to β-catenin shuttling out of the nucleus for ubiquitin-dependent degradation and constrained tumor growth. Further, RNA-sequencing of amassed *FAT4*-KO cells identified activation of WNT5A and ROR2. The noncanonical WNT5A/ROR2 signaling has no effect on β-catenin and its target genes (CCND1 and c-Myc) expression. Instead, we observed downregulation of receptors for WNT/β-catenin signaling, suggesting the shifting of β-catenin-dependent to β-catenin-independent pathways as tumor progression depends on its receptor expression. Both PAK6 and WNT5A could induce the expression of

Abbreviations: α-SMA, α-smooth muscle actin; 5′-aza-dC, 5-azadeoxycytidine; CCND1, Cyclin D1; COL1A1, collagen type 1; E-cad, E-cadherin; ECM, extracellular matrix; EMT, epithelial-mesenchymal transition; DEG, differential gene expressions; FAT4, FAT atypical cadherin 4; FAT4-KO, knockout FAT4; FN1, fibronectin; GO, Gene Ontology; ITGBI, integrin β1; LAMA4, laminin subunit alpha 4; MAPK, Mitogen-activated protein kinase; NCBI GEO, National Center for Biotechnology Information Gene Expression Omnibus; P13K-Akt, Phosphoinositide 3-kinase (PI3K)/protein kinase B (Akt); PAK6, p21 (RAC1)-activated kinase 6; RNA, seq, RNA-sequencing; ROR2, Receptor tyrosine kinase-like orphan receptor 2; WNT, Wingless-type; WNT5A, Wnt Family Member 5A; WT, wild-type.

Supplemental Digital Content is available for this article. Direct URL citations are provided in the HTML and PDF versions of this article on the journal's website, www.hepcommjournal.com.

extracellular matrix glycoprotein, laminin subunit alpha 4. Laminin subunit alpha 4 upregulation in HCC correlated with poor patient survival.

Conclusions: Our data show that FAT4 loss is sufficient to drive HCC development through the switching of canonical to noncanonical Wingless-type signaling pathways. The findings may provide a mechanistic basis for an in-depth study of the two pathways in the early and late stages of HCC for precise treatment.

INTRODUCTION

Wound-healing response to chronic liver injury results in excessive accumulation of extracellular matrix (ECM) and fibrosis. This ultimately disrupts proper functioning of the liver and establishes cirrhosis,[1] and may eventually progress to HCC.[2] Myofibroblasts are the major cells responsible for the deposition of collagen and other ECM proteins in tissue repair processes and liver fibrosis.[3] Hepatic stellate cells, bone marrow-derived fibroblasts, portal fibroblasts, hepatocytes, and bile duct cells can undergo epithelial-mesenchymal transition (EMT), giving rise to myofibroblasts and contributing to liver fibrosis.[4,5] EMT is a process by which epithelial cells lose their apical-basal polarity and cell-cell adhesion and acquire myofibroblastic features, including enhanced motility.[6] These cells may transform into tumor cells that can later acquire malignant phenotypes.[7]

Wingless-type (WNT) signaling regulates a wide range of biological events, such as cell fate determination, cell polarity, cell migration, and organ development.[8] The WNT signaling is mainly divided into the canonical β-catenin-dependent pathway and the noncanonical Ca^{2+} or planar cell polarity (PCP) pathways.[9] The canonical WNT/β-catenin pathway activates target gene transcription, which in turn regulates cell proliferation, behavior, and survival.[10] The noncanonical WNT/Ca^{2+} or WNT/PCP pathways mostly function in controlling cell polarity and migration.[10] Dysregulation of WNT signaling has been involved in EMT induction and pathophysiology of liver fibrosis.[11,12] Although the functional roles of many components of the WNT pathways have been characterized, the precise mechanism that regulates the WNT signaling in the initiation and progression of liver fibrogenesis remains unknown. Further studies on how normal cells undergo EMT and ECM synthesis and participate in fibrosis and HCC development may delineate the regulatory mechanisms of WNT signaling pathways in liver fibrogenesis. This may also provide important clues to how chronic liver disease progresses to HCC, leading to the identification of new therapeutic targets in liver fibrosis.

FAT atypical cadherin 4 (FAT4) is a member of the cadherin superfamily that regulates PCP and cell adhesion.[13] Mutation screening studies show that FAT4 is recurrently mutated in several types of human cancers, including HCC.[14–16] Expression analysis also suggests that FAT4 plays a tumor suppressor role in HCC and other cancers.[14–17] Silencing of FAT4 has been found to induce EMT and promote cell growth and invasion through the activation of Wnt/β-catenin signaling in gastric, colorectal, and ovarian cancers.[18–20] These observations imply a possible role of FAT4 in the WNT signaling pathways leading to HCC. However, whether loss of FAT4 in adherens junctions disrupts polarized hepatocyte layers and promotes cell transdifferentiation, which contributes to liver fibrosis and tumorigenesis, remains unknown.

In this study, we aimed to determine the functional role of FAT4 in hepatocarcinogenesis and identify its possible correlation with the WNT signaling pathways. Determining their roles in hepatocytes transdifferentiation, tumor initiation and progression may provide important clues to how chronic liver disease initiates the development and progression of HCC.

METHODS

Clinical specimens and cell lines

Thirty paired tumor and adjacent nontumor liver tissues were obtained from patients who had HCC and had undergone surgical resection at the Queen Mary Hospital, Hong Kong. Sample collection procedures and clinicopathological parameters were described in our previous study.[21] Liver biopsies obtained from 9 patients without HCC were included as controls. The study was approved by the Institutional Review Board of the University of Hong Kong (UW 19-747). Five human liver cancer cell lines (HepG2, HepG2.2.15, SNU-387, Huh7, and Hep3B) were obtained from the American Type Culture Collection (Manassas, VA, USA). The nontransformed hepatic cell line, L02 was obtained from the Shanghai Institutes for Biological Sciences and the Chinese Academy of Sciences. Cells were maintained in RPMI-1640 medium with 10% fetal bovine serum (Thermo Fisher Scientific, MA, USA) in a humidified incubator with 5% CO_2 at 37°C.

Quantitative methylation-specific PCR

Genomic DNA (1 μg) was subjected to bisulfite conversion by using the Ez DNA Methylation Gold Kit (Zymo Research, CA, USA) as per the manufacturer's instructions. The methylation status of the 13 CpG sites on the FAT4 promoter was investigated with primers specific to the methylated sequence [M-methylation-specific PCR (MSP)] and primers for both methylated and unmethylated sequences (U-MSP) (Supplemental Figure 1A-B, http://links.lww.com/HC9/A691). The reference methylated DNA was prepared by methylation of the fully unmethylated DNA with SssI methylase (New England Biolabs, Cambridge, UK). Quantitative MSP was conducted with SYBR Green I (Roche) in the CFX Connect™ real-time PCR system (Bio-Rad Laboratories, CA, USA). Temperatures that allow specific annealing were determined with fully methylated and unmethylated DNA. The percentage of methylated reference values was calculated as the fraction of the methylated reference.[22]

Demethylation and bisulfite sequencing

Promoter methylation of the liver cell lines was analyzed by q-MSP and quantified by bisulfite sequencing. To confirm whether epigenetic alteration silences FAT4 expression, Hep3B and Huh7 cells were incubated in media containing demethylating agent 5-azadeoxycytidine (5′-aza-dC; Sigma-Aldrich) for 3 days. 100 nM of histone deacetylating agent, trichostatin A (TSA; Sigma-Aldrich) was added to the medium alone or with 5′-aza-dC on day 3. Expression of FAT4 mRNA was analyzed by quantitative polymerase chain reaction (qPCR) as described. Primer sequences used for gene amplification are listed in Supplemental Table 1, http://links.lww.com/HC9/A691.

CRISPR/Cas9-mediated gene knockout

CRISPR/Cas9 system-mediated gene knockout was performed as described[23] using the FAT4 human gene KO kit (Origene). Briefly, L02 cells (3×10^5) were seeded in a 6-well plate and transfected with the guide and donor vectors using the Lipofectamine® 3000 reagent (Thermo Fisher Scientific) according to the manufacturer's instructions. The guide vector contains a single-guide RNA sequence and the donor contains sequences for puromycin resistance and green fluorescent protein. Two single-guide RNA sequences were used in this study and the sequences are listed in Supplemental Table S1, http://links.lww.com/HC9/A691. High green fluorescent protein expression cells were sorted into a 96-well plate using the automated cell sorter (BD Biosciences FACS Aria II, USA). The single clone was expanded and confirmed for FAT4-KO before being used for later experiments.

Stable shRNA-mediated PAK6 transfection

For stable clone generation, L02 cells with *FAT4*-KO were transfected with 2 μg of p21 (RAC1)-activated kinase 6 (PAK6)–specific shRNA or negative control shRNA (Origene) using Lipofectamine™ 3000. Stable clones were selected in 2 μg/ml puromycin for 4 weeks, and a single clone was isolated using a limited dilution technique.

Xenograft tumor formation in mice

BALB/c-nude mice (4-week-old) were subcutaneously inoculated with 5×10^6 of the indicated cells. Tumor growth was monitored every 3 days, and the tumor volume was calculated using the formula: $V = 1/2$ (length $\times$ width^2). All animal experiments were approved by the Committee on the Use of Live Animals in Teaching and Research (CULATR) of our institute.

Cell fractionation

Cells were suspended in 300 μl of extraction buffer containing 250 mM sucrose, 10 mM HEPES, pH 7.4, 0.5 mM DTT, 5 mM $MgCl_2$, 0.5% Nonidet P-40, and a mixture of protease inhibitors (Roche Diagnostics). Cells were disrupted with a glass Dounce homogenizer before being centrifuged at 12,000 rpm for 5 minutes. The supernatant was designated and cytoplasmic fraction was collected. Cell pellets were resuspended in 150 μl of prechilled nuclear lysis buffer containing 20 mM HEPES, pH 7.9, 1.5 mM $MgCl_2$, 0.5 M NaCl, 0.2 mM EDTA, and 20% glycerol. After centrifugation at 12, 000 rpm for 10 minutes, the nuclear fraction supernatant was collected.

Statistical analysis

Continuous variables were expressed as mean ± SEM and analyzed using the Student's *t*-test. All statistical analyses were performed using GraphPad Prism 5.0 (GraphPad Software, San Diego, CA). A *p*-value of less than 0.05 was considered statistically significant.

Additional methods

Detail methods for nucleic acid extraction, real-time PCR, immunofluorescence, siRNA transfection, cell proliferation, western blotting, RNA-sequencing (RNAseq) and

bioinformatics analyses, and cell migration and invasion assays are available in Supplemental Materials and Methods, http://links.lww.com/HC9/A692.

RESULTS

FAT4 is downregulated in HCC by epigenetic alterations

We first examined the methylation status in 13 CpG sites at the *FAT4* promoter region in liver tissues. As shown in Figure 1A, the percentage of methylated reference score in HCC tissues (9.8 ± 3.1) was significantly higher than their peritumor counterparts (3.6 ± 0.5) and noncancerous liver biopsies (0.3 ± 0.1) (both $p < 0.0001$). Peritumor tissues also showed a significantly higher percentage of methylated reference score than noncancerous liver biopsies ($p < 0.0001$). We next determined FAT4 expression in the same set of tissues. As shown in Figure 1B, FAT4 expression was significantly downregulated in HCC tissues when compared with their peritumor counterparts and noncancerous liver biopsies (both $p < 0.0001$). Specifically, downregulation of FAT4 was observed in 70% (21 out of 30) of HCC tissues compared with their peritumor counterparts (Figure 1C). Expression of FAT4 in peritumor tissues was also significantly lower than noncancerous biopsies ($p < 0.0001$) (Figure 1B). An inverse correlation between FAT4 promoter methylation and gene expression in HCC tissues was observed ($r = -0.622$, $p < 0.0001$) (Figure 1D).

To corroborate that the downregulation of FAT4 expression was caused by epigenetic alterations in HCC, we analyzed the promoter methylation of FAT4 in 5 HCC cell lines (Hep3B, Huh7, HepG2, HepG2.2.15, and SNU-387) and the nontransformed liver cell line L02. Methylation at the FAT4 promoter region was not detected in L02 cells (Figure 1E and Supplemental Figure 1C, http://links.lww.com/HC9/A691), but was found in all five cancer cell lines (Figure 1E). Treatment of the 2 densely methylated HCC cell lines Huh7 and Hep3B with 500 nM or 1 μM demethylating agent (5′-aza-dC) reversed methylation and restored FAT4 expression (Figure 1F and Supplemental Figure 1C, http://links.lww.com/HC9/A691). We also determined whether histone modification was involved in the silencing of FAT4 expression; Huh7 and Hep3B cells were treated with 100 nM histone deacetylase inhibitor (TSA). As shown in Figure 1F, TSA treatment increased FAT4 mRNA expression in both cell lines, though a significant increase in gene expression was only observed in Huh 7 cells ($p < 0.05$). Combined treatment of cells with 100 nM TSA and 1 μM 5′-aza-dC further enhanced FAT4 expression (Figure 1F). These findings confirmed that both DNA methylation and histone modification were involved in the downregulation of FAT4 expression in HCC.

Knockout of FAT4 drives morphologic changes and epithelial-to-mesenchymal transition

We used the CRISPR/Cas9 system to generate FAT4 knockout (FAT4-KO) in L02 cells to elucidate the mechanisms underlying the functional role of FAT4 in HCC (Supplemental Figure 2, http://links.lww.com/HC9/A691). Junction PCR amplification was performed to confirm integration at the FAT4 genomic target site (Supplemental Figure 2A-B, http://links.lww.com/HC9/A691). The absence of FAT4 expression in *FAT4*-KO cells was confirmed at mRNA and protein levels, respectively (Supplemental Figure 2C-D, http://links.lww.com/HC9/A691). Notably, changes in cell morphology were observed after *FAT4*-KO. The uniform and compact L02 *FAT4* wild-type (WT) cells were transformed into elongated, spindle-like motile cells and lost cell-cell adhesion (Supplemental Figure 2E, http://links.lww.com/HC9/A691). The *FAT4*-WT cells appeared to undergo EMT to have the characteristics of motile cancer cells after *FAT4*-KO. To determine whether molecular alterations associated with EMT also occurred upon the loss of FAT4, we assessed the protein expression of EMT markers in *FAT4*-WT and *FAT4*-KO cells by immunofluorescence (Figure 2). Compared with *FAT4*-WT cells, the mean fluorescence intensity of epithelial cell markers E-cadherin (E-cad) and zonula occludens-1 (ZO-1) was significantly reduced (1.88-fold and 2.1-fold decreases; both $p < 0.0001$) (Figure 2A, B), while the mean fluorescence intensity of mesenchymal cell markers vimentin and N-cadherin was significantly increased (2.88-fold and 6.29-fold increases; both $p < 0.0001$) (Figure 2D, E) in *FAT4*-KO cells. The altered expression of EMT markers was further confirmed by western blot. Similarly, the epithelial proteins E-cad and ZO-1 were downregulated, while the mesenchymal proteins vimentin and N-cadherin were upregulated in *FAT4*-KO cells compared with the control *FAT4*-WT cells (Figure 2C, F). These observations suggested that FAT4 is a member of the cadherin gene superfamily, and it may also protect hepatocytes from the loss of cell-cell adhesion and undergoing transdifferentiation.

Loss of FAT4 induces extracellular matrix synthesis, cell migration, and invasion

Alterations in ECM composition are involved in EMT and cancer progression. Thus, we determined the expression of the major ECM components fibronectin (FN1) and integrin β1 (ITGB1) by immunofluorescence. As shown in Figure 3A, significant increases in FN1 and ITGB1 protein expressions were found in *FAT4*-KO cells compared with control *FAT4*-WT cells (5.09-fold and 5.14-fold increases in fluorescence intensity, respectively; both $p < 0.0001$).

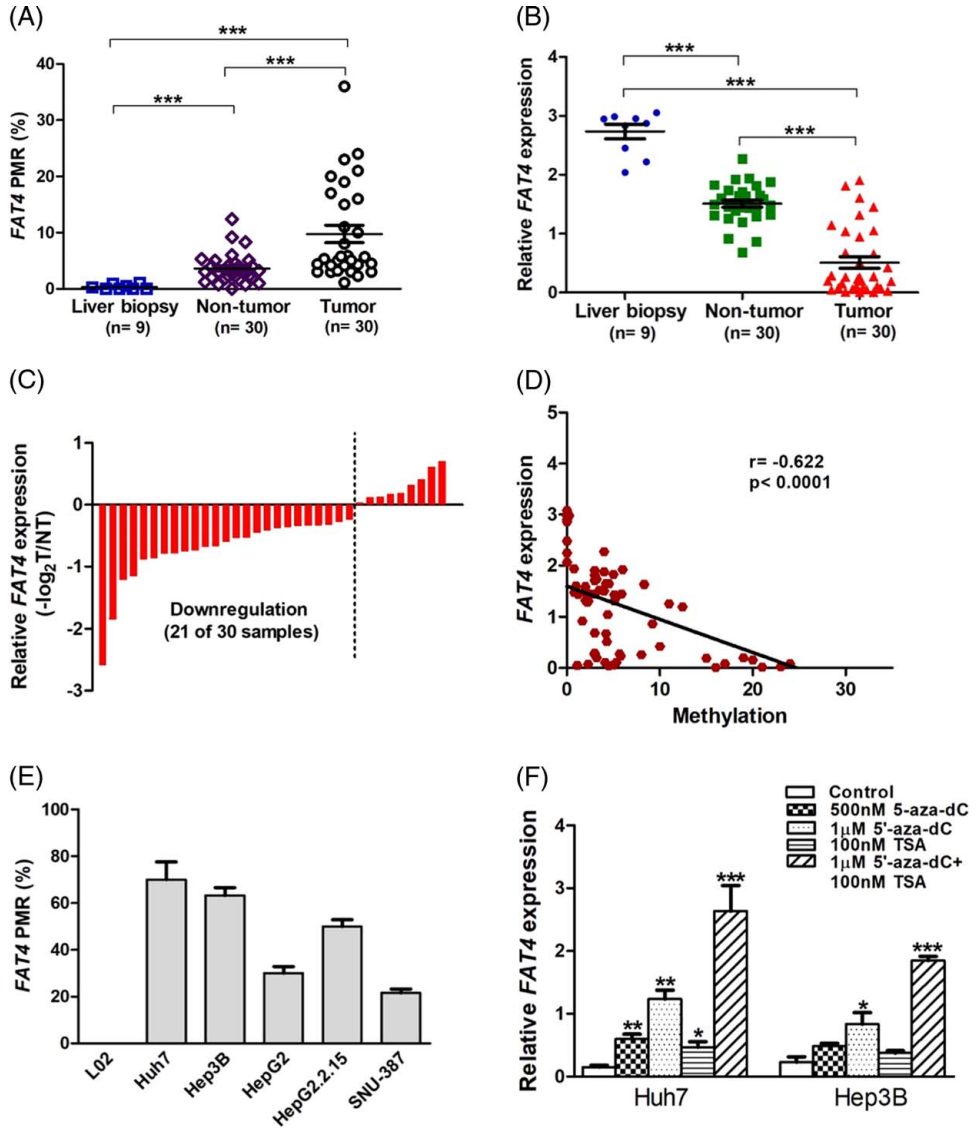

FIGURE 1 Epigenetic inactivation of FAT4 in HCC. (A) FAT4 promoter methylation was investigated by quantitative methylation-specific PCR (q-MSP). The PMR value for each sample was calculated as the fraction of the reference. (B) qPCR measurement of FAT4 mRNA expression in noncancerous liver biopsies and HCC and their adjacent nontumor tissues. (C) Waterfall plot demonstrating the downregulation of FAT4 expression in HCC tissues compared with their adjacent nontumor tissues. (D) Correlation of FAT4 promoter methylation and gene expression. (E) q-MSP analysis of FAT4 promoter methylation in normal liver cell line L02 and five HCC cell lines. (F) FAT4 mRNA expression in Huh7 and Hep3B cells was restored with 5′-aza-dC (500 nM and 1 μm) and TSA (100 nM) treatment. FAT4 mRNA expression was further restored with combined 5′-aza-dC (1 μM) and TSA (100 nM) treatment. Data are shown as the mean ± SEM. Statistically significant differences are denoted by asterisks, ***$p < 0.0001$, **$p < 0.001$, *$p < 0.01$. Abbreviations: 5′-aza-dC, 5-azadeoxycytidine; PMR, percentage of methylated reference; q-MSP, quantitative methylation-specific polymerase chain reaction; TSA, trichostatin A.

Downregulation of E-cad during EMT will disrupt the binding of E-cad to β-catenin in the cytoplasm. As shown in Figure 3B, immunofluorescence staining showed nuclear translocation of β-catenin in *FAT4*-KO cells compared with cytoplasmic β-catenin expression in control cells. Interestingly, western blot analysis showed that *FAT4*-KO also increased β-catenin expression (Figure 3C) as well as its target genes FN1 and ITGB1. These findings suggest that *FAT4*-KO activates β-catenin nucleus translocation and induces ECM synthesis.

To further validate our hypothesis that *FAT4*-KO induces cell transdifferentiation via EMT leading to the generation of ECM-producing myofibroblasts, we detected the expression of myofibroblast markers α-smooth muscle actin (α-SMA) and collagen type 1 (COL1A1). As shown in Figure 3D, immunofluorescence staining indicated cell transdifferentiation marked by the detection of α-SMA and COL1A1 proteins in *FAT4*-KO cells. Similarly, expressions of α-SMA and COL1A1 proteins were detected by western blot in *FAT4*-KO cells but not in control *FAT4*-WT cells (Figure 3E).

We next determined whether the observed β-catenin translocation in *FAT4*-KO cells induced cell growth and

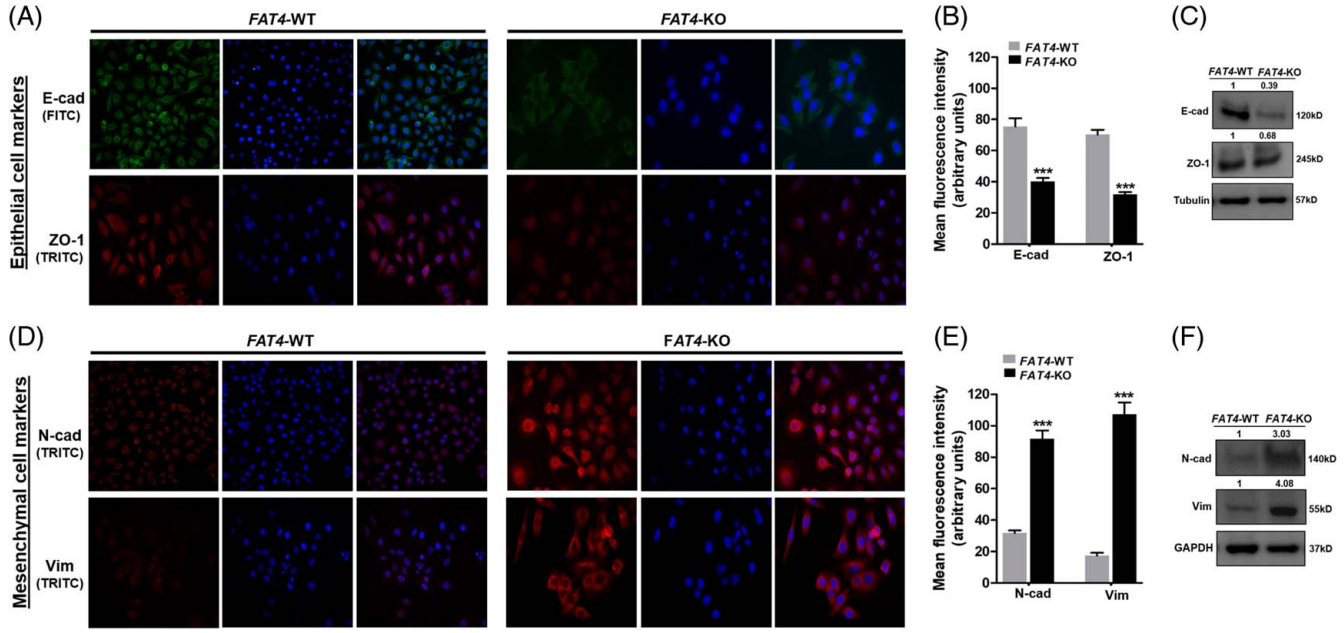

FIGURE 2 Knockout of *FAT4* induces EMT in the nontransformed hepatic cell line L02. (A) Immunofluorescence staining of epithelial cell markers E-cad and ZO-1 in L02 *FAT4*-WT and *FAT4*-KO cells. (B) Fluorescence intensity quantification showing that E-cad and ZO-1 was significantly reduced in *FAT4*-KO cells. (C) Western blot analysis indicated the downregulation of E-cad and ZO-1 proteins in *FAT4*-KO cells. (D) Immunofluorescence analysis of mesenchymal markers N-cad and Vim in L02 *FAT4*-WT and *FAT4*-KO cells. The fluorescence intensity of N-cad and Vim proteins was significantly increased in *FAT4*-KO cells compared with control *FAT4*-WT cells. The protein expression of mesenchymal markers N-cad and Vim was upregulated in *FAT4*-KO cells. Magnification: 400x. Blue: DAPI. All error bars show the SEM. ***$p < 0.0001$.Abbreviations: E-cad, E-cadherin; FAT4-KO, knockout FAT4; EMT, epithelial-mesenchymal transition; N-cad, N-cadherin; Vim, Vimentin; ZO-1, zonula occludens-1.

invasion. As shown in Figure 3F, *FAT4*-KO significantly enhanced cell proliferation at the 3 time points measured when compared with control *FAT4*-WT cells ($p < 0.01$ at 24 hours, and $p < 0.0001$ at both 48 and 72 hours). The effects of *FAT4*-KO on cell motility were assessed using the scratch assay. Wound closure was significantly faster in *FAT4*-KO cells, with 95% of the area healed in *FAT4*-KO cells than 37% in control cells at 48 hours ($p < 0.0001$) (Figure 3G). We further explored the role of FAT4 in cell migration and invasion. *FAT4*-KO significantly promoted cell migration, as denoted by the increase in cell colonies when compared with control cells (146.3 ± 12.8 vs. 57.0 ± 5.1, $p < 0.0001$) (Figure 3H). Of note, using the matrigel-coated invasion chamber, only *FAT4*-KO cells invaded through the matrix, but not the control *FAT4*-WT cells (Figure 3H). These results suggest that loss of FAT4 activated WNT/β-catenin signaling, which promotes tumor growth and invasion.

RNA-sequencing analysis identifies gene expression changes following FAT4 knockout

RNAseq was performed to profile differential gene expressions (DEGs) in FAT4-KO cells. As shown in Figures 4A and B, out of 21732 variables, 298 DEGs ($\log_2$ fold change > 2, false discovery rate <0.05) were identified, with 187 upregulated and 111 downregulated in the *FAT4*-KO cells compared with the *FAT4*-WT controls (Supplemental File 1, http://links.lww.com/HC9/A693). Kyoto Encyclopedia of Genes and Genomes pathway enrichment analysis revealed that the most enriched pathways were PI3K-Akt signaling pathway, ECM-receptor interaction, focal adhesion, and MAPK signaling (Figure 4C and Supplemental File 2, http://links.lww.com/HC9/A694). These pathways are crucial for cell binding and adhesion, and are involved in tumor invasion and metastasis.[24] The function of the DEGs was further classified using the Gene Ontology (GO) classification system, which defined genes according to molecular function, cellular component, and biological process. Figure 4D shows the top 10 most enriched GO terms in each category. Most of the genes function in binding, extracellular matrix, and regulation of signaling and development.

Multiple analyses indicated that most DEGs were enriched in adhesion, PI3K-Akt signaling, ECM-receptor interaction, and MAPK signaling pathways. Candidate DEGs from these identified pathways are displayed on the heat map (Figure 4E and Supplemental File 2, http://links.lww.com/HC9/A694). As shown in Figure 4F, candidate genes that function as collagen, integrin, and growth factors from these pathways were selected for further qPCR validation. The results of qPCR confirmed that the expression trends of these DEGs coincided with the RNA-seq results (Figure 4E), which

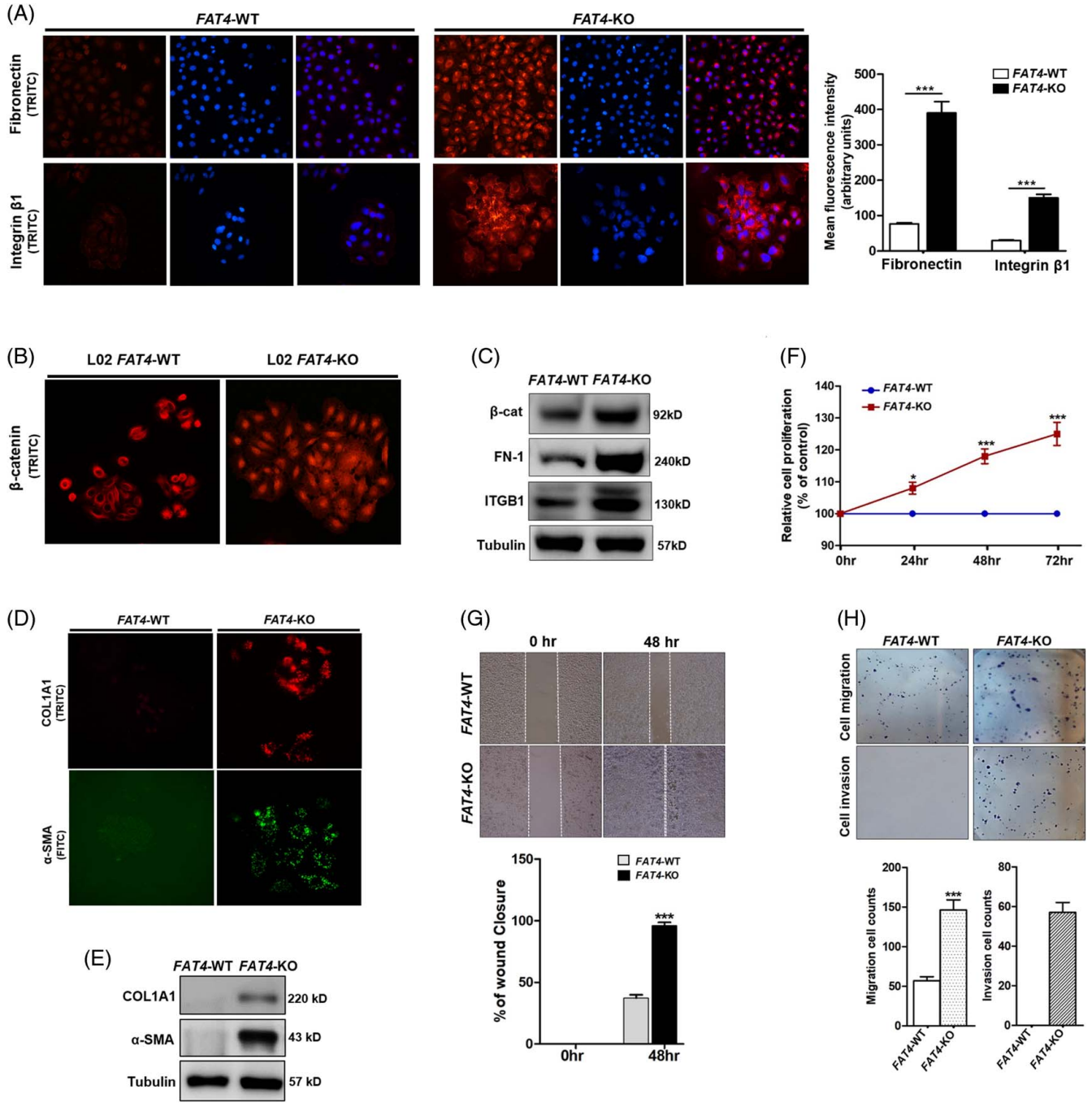

FIGURE 3 Loss of *FAT4* induces ECM deposition, transdifferentiation, and cell migration and invasion. (A) Immunofluorescence staining of major ECM components FN1 and ITGB1. Measurement of fluorescence intensity showed a significant increase in FN1 and ITGB1 expressions in *FAT4*-KO cells compared with *FAT4*-WT controls. (B) Immunofluorescence staining shows activation and nuclear translocation of β-cat in *FAT4*-KO cells compared with cytoplasmic β-cat expression in *FAT4*-WT cells. (C) Western blot analysis demonstrated upregulation of ECM proteins β-cat, FN1, and ITGB1 in *FAT4*-KO cells compared with *FAT4*-WT cells. (D-E) Immunofluorescence staining and western blot indicated cell transdifferentiation, which was marked by increased α-SMA and COL1A1 proteins' expression in *FAT4*-KO cells. (F) *FAT4*-KO significantly increased cell proliferation. (G) *In vitro* wound-healing assay demonstrates that *FAT4*-KO significantly enhanced cell migration. (H) Transwell invasion assay also shows the increased migration and invasion potential of *FAT4*-KO cells. All error bars show the SEM. *$p < 0.1$ and ***$p < 0.0001$. Abbreviations: α-SMA, α-smooth muscle actin; β-cat, β-catenin; COL1A1, collagen type 1; ECM, extracellular matrix; FAT4-KO, knockout FAT4; FN1, fibronectin; ITGB1, integrin β1.

provides valuable information for the downstream analysis. Of note, we found that PAK6, which functions in the focal adhesion pathway, was significantly upregulated in *FAT4*-KO cells (Figures 4A, 4E, and 4F).

PAK6 promotes *in vivo* tumor growth and progression in *FAT4*-KO cells

We next examined the effects of *FAT4*-KO and PAK6 knockdown on tumor growth *in vivo*. When inoculated into

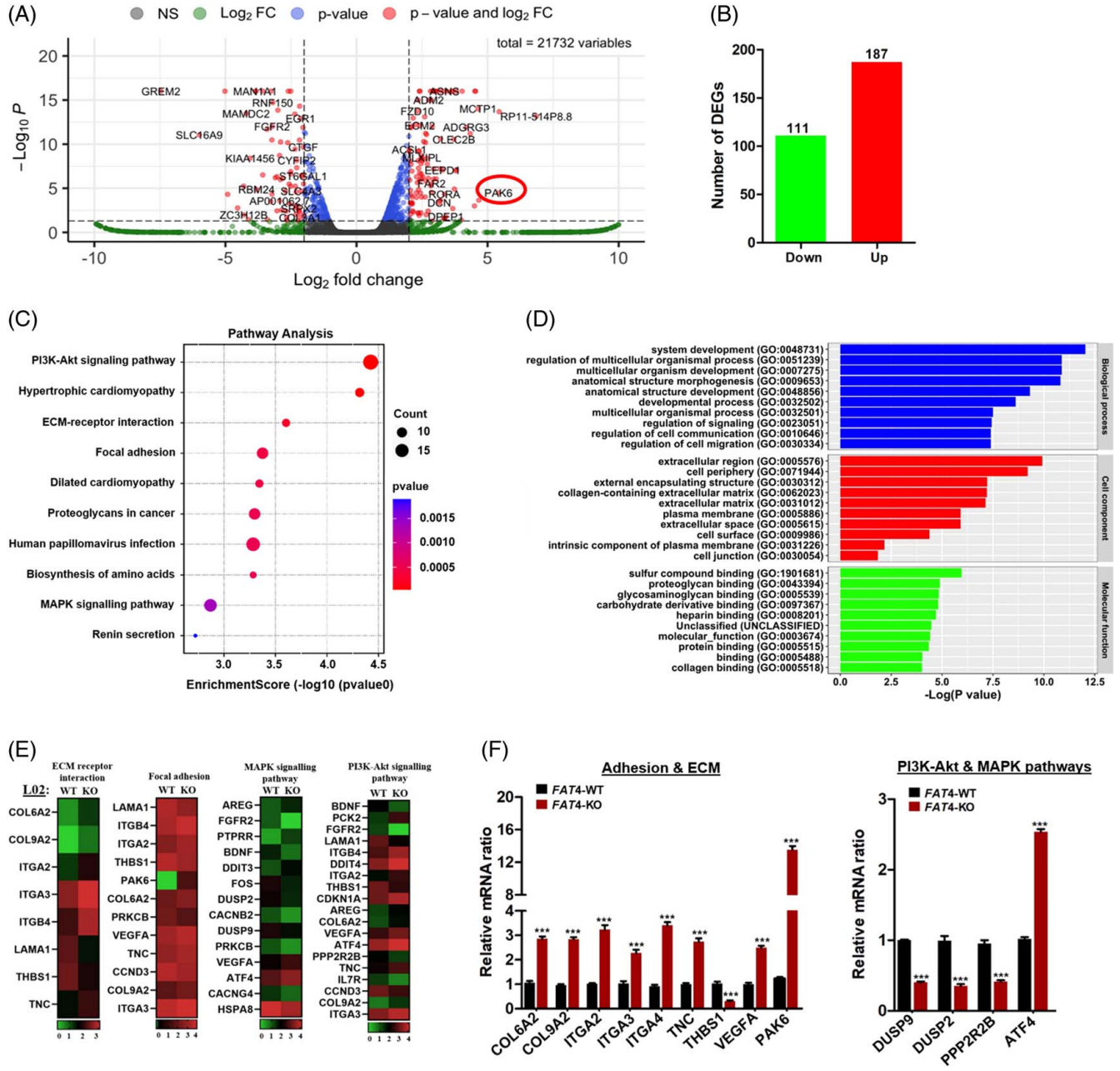

FIGURE 4 RNA-seq analysis of gene expression changes in nontransformed human hepatic cell line L02 with or without *FAT4*-KO. (A) Volcano plot illustrating differential gene expression identified by RNA-seq. Genes with Log_2 fold change > 2 (red) or <-2 (blue) and adjusted with FDR < 0.05 were defined as DEGs. (B) Bar plot showing the number of upregulated and downregulated genes in the *FAT4*-KO cells compared with *FAT4*-WT controls. (C) Bubble diagram showing the top 10 pathways involved in *FAT4*-KO identified from KEGG pathway enrichment analysis of DEGs. The color of the spots indicates the *p*-value, and the size of the dots corresponds to the number of genes annotated. (D) The top 10 most enriched GO terms found in the analysis of DEGs in *FAT4*-KO versus *FAT4*-WT cells. Different colors represent biological processes, molecular functions, and cellular components. (E) Heat map showing representative DEGs in the pathways in *FAT4*-WT versus *FAT4*-KO cells. The red color denotes the upregulation of DEGs, and the green color denotes the downregulation of DEGs. (F) Expression of representative genes from the selected functional pathways was validated by qPCR. Data represent means ± SEM. ***$p < 0.0001$. Abbreviations: DEG, differentially expressed genes; FAT4-KO, knockout FAT4; FDR, false discovery rate; *FAT4,* FAT atypical cadherin 4; KO, knockout; KEGG, Kyoto Encyclopedia of Genes and Genomes; GO, gene ontology; qPCR, quantitative polymerase chain reaction.

nude mice, *FAT4*-KO cells were able to give rise to tumors in all cases (n = 10), while the control *FAT4*-WT cells were unable to form tumors (n = 10) (Figure 5A). Two out of the 10 mice inoculated with *FAT4*-KO cells developed hepatic metastasis, with liver histology confirmed with hematoxylin-eosin staining (Figure 5B). Tumor formation ability was assessed by measuring the tumor volume and tumor weight. The tumor formation ability of *FAT4*-KO cells with PAK6 knockdown was significantly subdued when compared with control *FAT4*-KO cells with or without transfection with negative control-short hairpin RNA (Figure 5C-F). We also examined the expression of

proliferation marker Ki67 in xenograft tissue sections by immunohistochemistry. When compared with control *FAT4*-KO cells and *FAT4*-KO cells transfected with negative control-short hairpin RNA, xenografts generated from *FAT4*-KO cells with PAK6 knockdown displayed a reduction in Ki67 expression. These data confirmed our *in vitro* findings that cells acquired tumorigenic and metastatic potential after the loss of FAT4, and PAK6 was involved in tumor growth and progression.

PAK6 activates WNT/β-catenin signaling to promote tumor growth and progression

The alteration of PAK6 expression in human liver tissues was studied using data obtained from the NCBI GEO dataset (GSE25097). As shown in Figure 6A, HCC tissues had a significantly higher PAK6 expression than cirrhotic and normal liver tissues ($p < 0.01$ and $p < 0.001$, respectively). The expression of PAK6 in cirrhotic tissues was significantly higher than in normal liver tissues ($p < 0.001$). These results suggest that PAK6 overexpression maybe an early event in hepatocarcinogenesis.

Next, we determined whether PAK6 is involved in the nuclear translocation of β-catenin. As shown in Figure 6B, immunofluorescence staining showed β-catenin was shuttled out of the nucleus and aggregated in the cytoplasm in *FAT4*-KO cells transfected with PAK6-siRNA, while β-catenin was retained in the nucleus in *FAT4*-KO cells transfected with control siRNA. This result was confirmed by nucleocytoplasmic cell fractionation followed by Western blot analysis of phosphorylated β-catenin levels. As shown in Figure 6C, phospho-β-catenin was presented at higher levels in the cytoplasmic fraction than nuclear fraction in *FAT4*-KO cells transfected with PAK6-siRNA, indicating that β-catenin is phosphorylated at amino-terminal serine/threonine (Ser33/Ser37/Thr41) by glycogen synthase kinase 3β and targeted for ubiquitination, and subsequent proteasome degradation. Hence, we studied ubiquitination-dependent degradation of phosphorylated β-catenin in *FAT4*-KO cells with PAK6 knockdown. As shown in Figure 6D, PAK6 knockdown increased the expression of both glycogen synthase kinase 3β and phospho-β-catenin (Ser33/Ser37/Thr41). The augmented ubiquitination in *FAT4*-KO cells transfected with PAK6-siRNA was confirmed by both western blot analysis (Figure 6E) and immunofluorescence microscopy (Figure 6F), which showed an increased expression of ubiquitinated proteins and ubiquitin, respectively, in the PAK6 knockdown cells. We further determined the effects of PAK6 knockdown on the expression of two β-catenin target genes, namely CCND1 and c-Myc. As shown in Figure 6D, protein expression of CCND1 and c-Myc was reduced after PAK6 knockdown. These findings confirmed that PAK6 was involved in β-catenin activation, and PAK6 may promote tumor growth and progression in *FAT4*-KO cells through WNT/β-catenin signaling.

RNA-seq analysis of amassed cells to identify potential pathways in tumor dissemination

We observed that *FAT4*-KO cells could grow and amass more cells over a period of 12 days (Figure 6G), as opposed to the nontransformed *FAT4*-WT cells, which exhibited cell-cell contact inhibition on day 12 (Figure 6G). It remains obscure for how transformed cells grow and become invasive; we thus performed RNA-seq analysis on cells isolated from the clonal population (L02 *FAT4*-KO-I). As shown in Figures 7A and B, of the 22377 variables, 526 DEGs ($\log_2$ fold change >2, false discovery rate <0.05) were identified, with 283 upregulated and 243 downregulated in the L02 *FAT4*-KO-I cells compared with the *FAT4*-KO controls (Supplemental File 3, http://links.lww.com/HC9/A695). The top 10 enriched pathways obtained from the Kyoto Encyclopedia of Genes and Genomes pathway enrichment analysis revealed that the DEGs were enriched in genes not only involved in the PI3K-Akt signaling pathway, ECM-receptor interaction, focal adhesion, and MAPK signaling but also in Hippo signaling pathway and WNT5A noncanonical signaling pathway (Figure 7C and Supplemental File 4, http://links.lww.com/HC9/A696). Similarly, these pathways are crucial for cell binding and adhesion, and are involved in tumor invasion and metastasis.

The function of the DEGs was classified using the GO classification system; Figure 7D shows the top 10 most enriched GO terms in each category. Most of the genes function for binding, extracellular matrix, and development. Candidate DEGs from the identified pathways are shown on the heat map (Figure 7E and Supplemental File 4, http://links.lww.com/HC9/A696). Genes were selected from these pathways for further qPCR validation. The results of qPCR confirmed that the expression trends of these DEGs coincided with the RNA-seq results (Figure 7F). Of note, we found that laminin subunit alpha 4 (LAMA4) functioning in the focal adhesion pathway was significantly upregulated in *FAT4*-KO-I cells (Figure 7A, E, and F). LAMA4 is an extracellular matrix glycoprotein, the exact function of which in HCC is still not clear.

Effects of PAK6 and WNT5A on LAMA4 expression

We then determined the clinical implication of LAMA4 expression in human liver tissues using the NCBI GEO dataset (GSE25097). As shown in Figure 8A, HCC tissues had a significantly higher LAMA4 expression than cirrhotic and normal liver tissues (both $p < 0.0001$). The expression of LAMA4 in cirrhotic tissues was

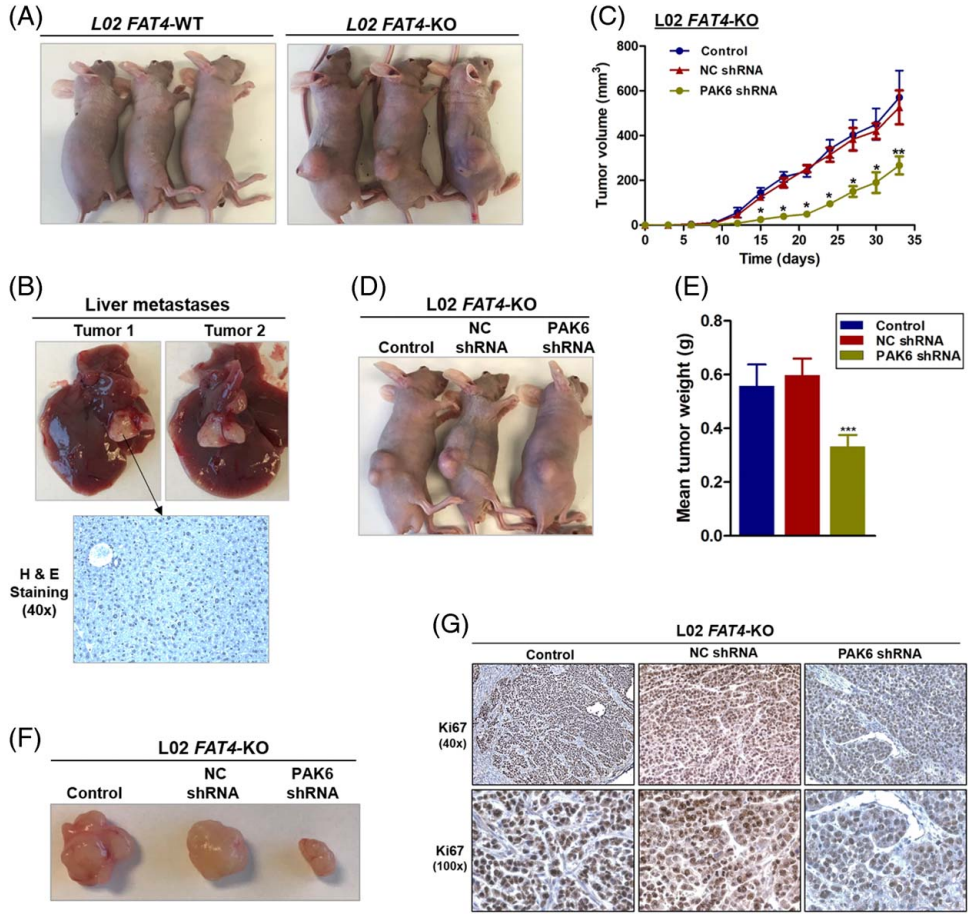

FIGURE 5 Knockout of FAT4 in the nontransformed human hepatic cell line L02 acquires tumorigenic and metastatic potential. (A) Representative pictures showing subcutaneous tumors in nude mice inoculated with L02 *FAT4*-KO cells. Tumors were initiated with inoculation of 5×10^6 *FAT4*-KO cells in mice (10/10). No tumor was found in control mice (0/10) inoculated with 5×10^6 *FAT4*-WT cells. (B) Liver metastases were found in mice (2/10) inoculated with *FAT4*-KO cells and liver histology was confirmed with H&E staining. (C) Tumor volume curves showing the growth of the tumors in nude mice inoculated with *FAT4*-KO cells and cells transfected with NC-shRNA or PAK6-shRNA. (D) Images showing the tumor-bearing mice in each treatment group. (E) The mean tumor weight of the resected tumors. L02 *FAT4*-KO cells with stable silencing of PAK6 significantly inhibited the growth of tumors in nude mice. (F) Images of the resected tumors after sacrificed at day 35. (G) Immunohistochemistry images of Ki67 staining in xenografts resected from mice inoculated with L02 *FAT4*-KO cells and cells transfected with NC-shRNA or PAK6-shRNA. *p* values were determined using Student's t-test. $^*p < 0.01$, $^{**}p < 0.001$, $^{***}p < 0.0001$. Abbreviations: FAT4, ;*FAT4*, FAT atypical cadherin 4; FAT4-KO, knockout FAT4; KO, knockout; H&E, hematoxylin-eosin; PAK6, p21 (RAC1)-activated kinase 6; NC-shRNA, negative control-short hairpin RNA.

significantly higher than in normal liver samples ($p < 0.001$). Using the TCGA-LIHC dataset, we found that there was a significant association between LAMA4 expression level and patient survival. Patients with higher LAMA4 expression had a poor overall survival than the patients with lower LAMA4 expression (Log-rank $p = 0.036$) (Figure 8B).

Since RNA-seq analysis demonstrated activation of WNT5A ligand in a noncanonical signaling pathway, we then evaluated whether the WNT5A noncanonical signaling pathway would regulate LAMA4 expression. As shown in Figure 8C, stimulation of L02 *FAT4*-KO-I cells with purified WNT5A at 15 or 30 ng/ml could activate LAMA4 expression in a dose-dependent manner. In addition, treatment of cells with purified WNT5A at 15 or 30 ng/ml also stimulated the noncanonical WNT5A/ROR2 signaling pathway, as reflected by an increase in protein expression of both genes (Figure 8C).

We had demonstrated that PAK6 was involved in WNT/β-catenin signaling, tumor growth, and progression. We next determined whether PAK6 affected LAMA4 expression. As shown in Figure 8D, PAK6 knockdown significantly reduced the expression of LAMA4 in L02 *FAT4*-KO-I cells compared with cells transfected with control siRNA. As expected, the addition of WNT5A significantly upregulated LAMA4 mRNA expression in L02 *FAT4*-KO-I cells. Knockdown of PAK6 reduced the stimulation effect of WNT5A on the activation of LAMA4 expression (Figure 8D). These data show that both PAK6 and WNT5A could modulate LAMA4 expression, and knockdown of PAK6 constrained the effect of WNT5A on the activation of LAMA4 expression.

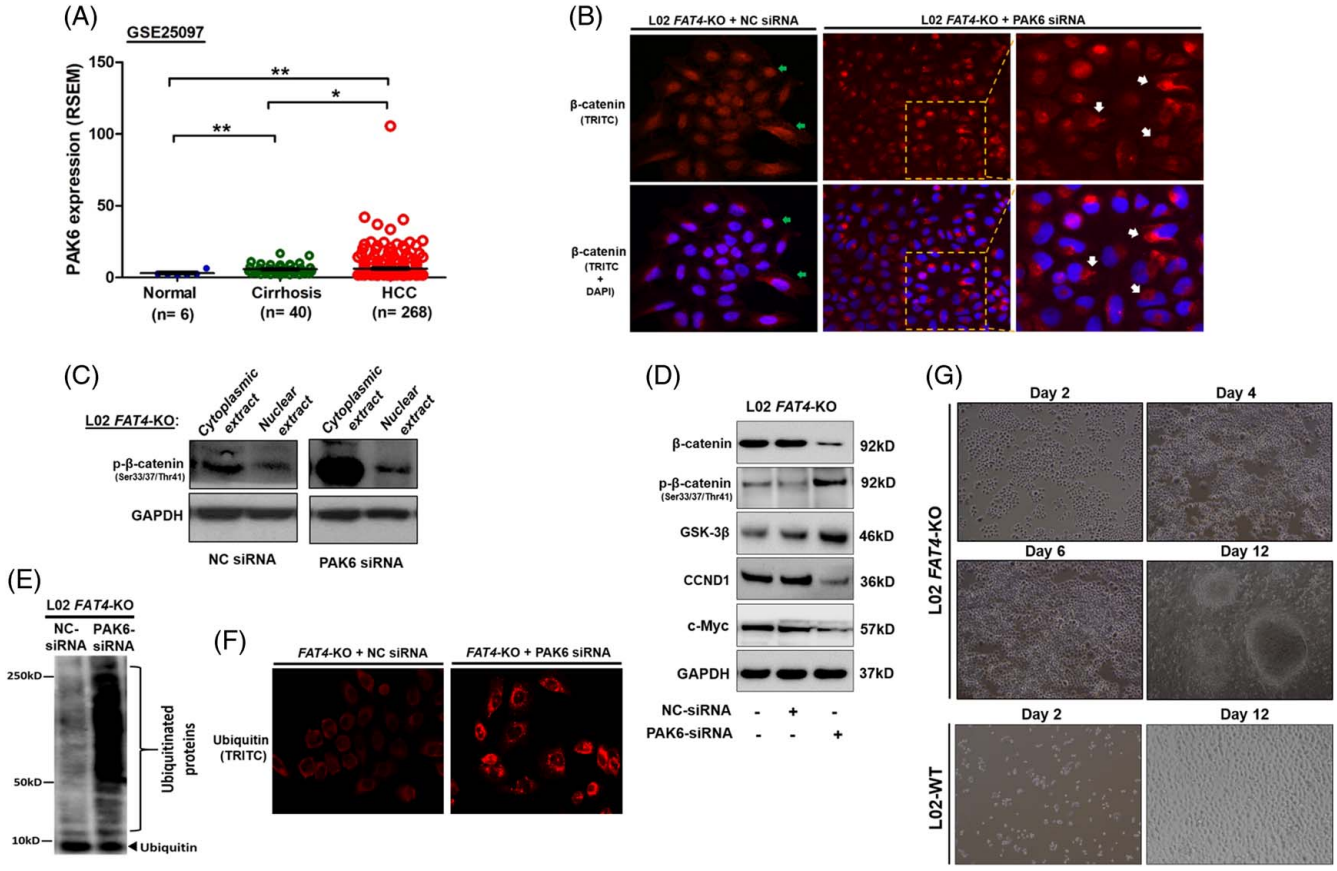

FIGURE 6 PAK6 involves in the nuclear translocation of β-catenin and is essential for tumor growth and progression. (A) qPCR analysis of PAK6 mRNA expression in normal liver biopsies, cirrhotic and HCC tissues using NCBI GEO dataset (GSE25097). (B) Immunofluorescence staining shows β-catenin shuttling out of the nucleus and aggregating in cytoplasm after PAK6 knockdown by siRNA in *FAT4*-KO cells. Green arrows indicate cytoplasmic staining while white arrows indicate nucleus staining. (C) Western blot analysis of phosphor-β-catenin protein in cytoplasmic and nuclear extracts of L02 *FAT4*-KO cells. (D) PAK6 knockdown increased GSK-3β and β-catenin phosphorylation, and suppressed transcription of β-catenin, CCND1, and c-Myc. (E) Western blot analysis of ubiquitinated proteins in L02 *FAT4*-KO cell lysates with or without PAK6 knockdown. (F) Immunofluorescence staining of ubiquitin in *FAT4*-KO cells with or without PAK6 knockdown. (G) Representative pictures showing the growth of normal L02 cells with contact inhibition and cancerous L02 *FAT4*-KO cells with cells amassed up over 12 days of culture (× 10 magnification). *$p < 0.01$, **$p < 0.001$. Abbreviations: CCND1, cyclin D1; *FAT4*, FAT atypical cadherin 4; FAT4-KO, knockout FAT4; GSK-3β, glycogen synthase kinase-3 beta; PAK6, p21 (RAC1)-activated kinase 6; qPCR, qPCR, quantitative polymerase chain reaction.

Activation of noncanonical WNT5A/ROR2 signaling pathway as tumor progresses

Previous reports have shown that noncanonical WNT ligands such as WNT5A might inhibit canonical WNT signaling.[25,26] We assessed the expression of β-catenin and its target genes CCND1 and c-Myc in the canonical pathway and WNT5A and its receptor ROR2 in the noncanonical pathway in *FAT4*-KO cells and *FAT4*-KO-I cells by western blot. As shown in Figure 8E, there was no difference in the protein expression of β-catenin and its target genes CCND1 and c-Myc between *FAT4*-KO cells and *FAT4*-KO-I cells. Instead, the expression of WNT5A and ROR2 in *FAT4*-KO-I cells was higher than in *FAT4*-KO cells. WNT5A does not inhibit canonical WNT/ β-catenin signaling in HCC cells. These findings suggest that the WNT5A/ROR2 noncanonical signaling is activated and involved in HCC progression.

DISCUSSION

In this study, we presented *in vivo* and *in vitro* experimental evidence to elucidate the mechanistic basis of FAT4 in the suppression of hepatocarcinogenesis. We first demonstrated that the downregulation of FAT4 in HCC was due to epigenetic alterations in the form of both promoter methylation and histone modification. These findings ascertain the tumor suppressor role of FAT4 in HCC and highlight that epigenetic hits also contributed to FAT4 inactivation.

We generated *FAT4*-KO in the normal hepatic cell line L02 to identify the underlying mechanism by which FAT4 functions to suppress hepatocarcinogenesis. Upon FAT4 knockout, epithelial L02 cells underwent EMT, lost cell-cell contacts, and acquired a mesenchymal-like phenotype, resulting in significantly enhanced cell proliferation, migratory capacity, and increased production of ECM components such as FN1 and ITGB1. Previous studies have reported

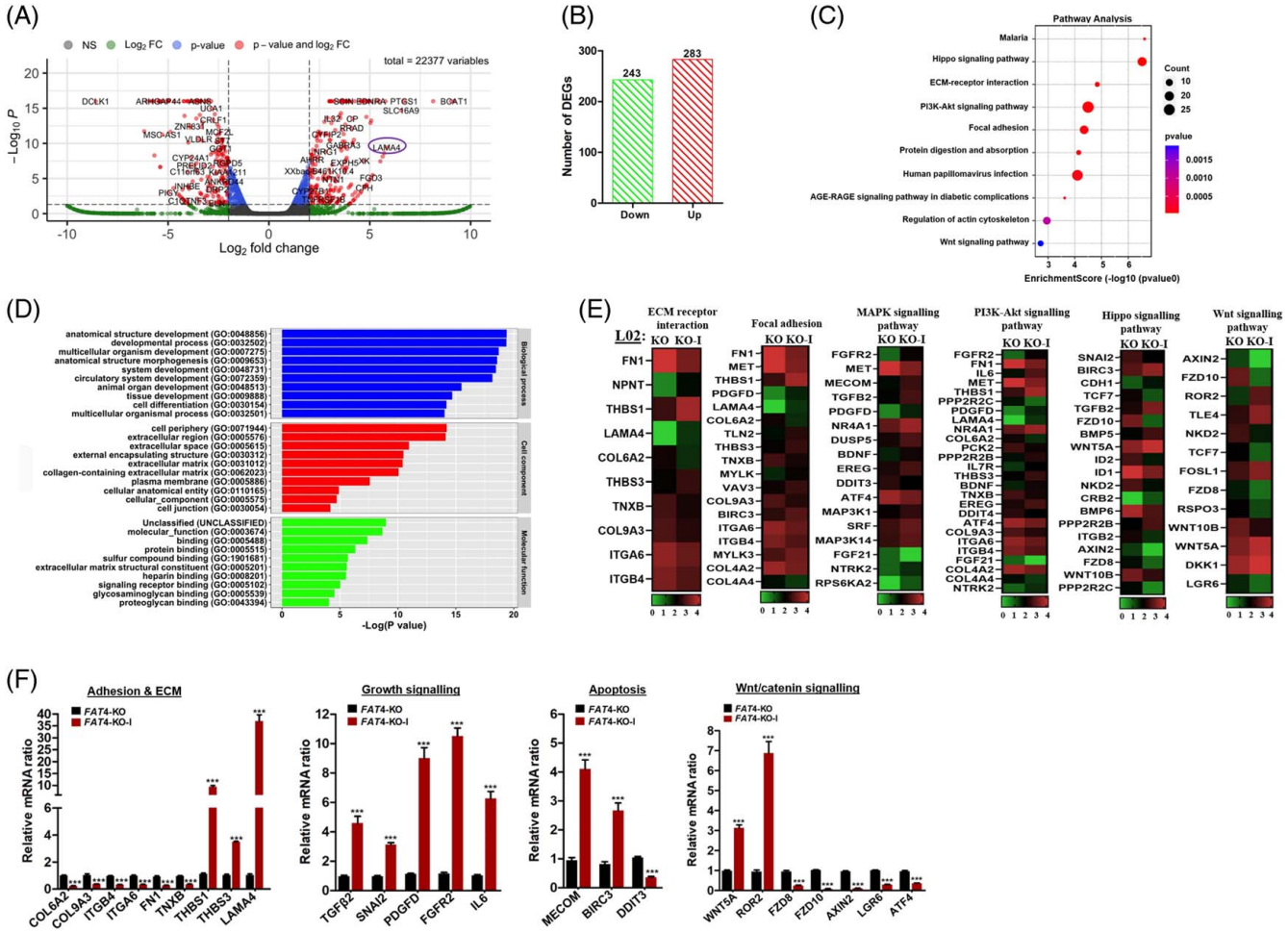

FIGURE 7 RNA-seq analysis of gene expression changes in amassed cells (L02 *FAT4*-KO-I) isolated from a 12-day culture of cancerous L02 *FAT4*-KO cells. (A) Volcano plot illustrating differential gene expression identified by RNA-seq. Genes with Log_2 fold change >2 (red) or <-2 (blue) and adjusted with FDR < 0.05 were defined as DEGs. (B) A total of 526 DEGs were identified, with 283 upregulated genes and 243 downregulated genes in the L02 *FAT4*-KO-I cells compared with *FAT4*-KO cells. (C) Bubble diagram showing the top 10 pathways involved in *FAT4*-KO-I cells identified from pathway enrichment analysis of DEGs. The color of the spots indicates the *p*-value, and the size of the dots corresponds to the number of genes annotated. (D) The top 10 most enriched GO terms found in the analysis of DEGs in *FAT4*-KO vs. *FAT4*-KO-I cells. Different colors represent biological processes, molecular functions, and cellular components. (E) Heat map showing representative DEGs in the pathways in *FAT4*-KO vs. *FAT4*-KO-I cells. The red color denotes the upregulation of DEGs, and the green color denotes the downregulation of DEGs. (F) Expression of representative genes from the selected functional pathways was validated by qPCR. Data represent means ± SEM. ***$p < 0.0001$. Abbreviations: DEG, differentially expressed genes; FDR, false discovery rate; GO, Gene Ontology; *FAT4*, FAT atypical cadherin 4; KO, knockout; qPCR, quantitative polymerase chain reaction; RNA-seq, RNA-sequencing.

that epithelial cells can acquire myofibroblastic phenotype through EMT and produce excessive ECM components, resulting in liver fibrosis.[3,4] In the present study, the transdifferentiation of *FAT4*-KO L02 cells to myofibroblasts was demonstrated by the detection of specific myofibroblastic cell markers α-SMA and COL1A1, as well as the mesenchymal cell markers vimentin and N-cadherin. Our data are in line with previous findings that hepatocytes can be a source of myofibroblasts and contribute to the synthesis of ECM and liver fibrogenesis.[27] Being a member of the cadherin superfamily, FAT4 is also involved in regulating cell adhesion and cell transformation, as demonstrated in our study. However, further *in vivo* and *in vitro* studies are warranted to elucidate the relative importance of FAT4 in hepatic fibrogenesis in order to decipher the complicated mechanisms of hepatic fibrogenesis, which may advance the development of antifibrotic drugs.

EMT is generally considered the primary process in driving tumor initiation and progression.[28] In this study, we found that *FAT4*-KO induced EMT and activated nuclear translocation of β-catenin. β-catenin nuclear translocation is a vital process of WNT/β-catenin signaling, which enhances tumor growth and invasion in some cancers, including HCC.[29] The causative role of WNT/β-catenin signaling on EMT with cell proliferation was confirmed by RNA-seq detection of PAK6 overexpression. Silencing of PAK6 suppressed tumor growth and progression in the xenograft model. Mechanistically, we found that the knockdown of PAK6 in *FAT4*-KO cells caused β-catenin to shuttle

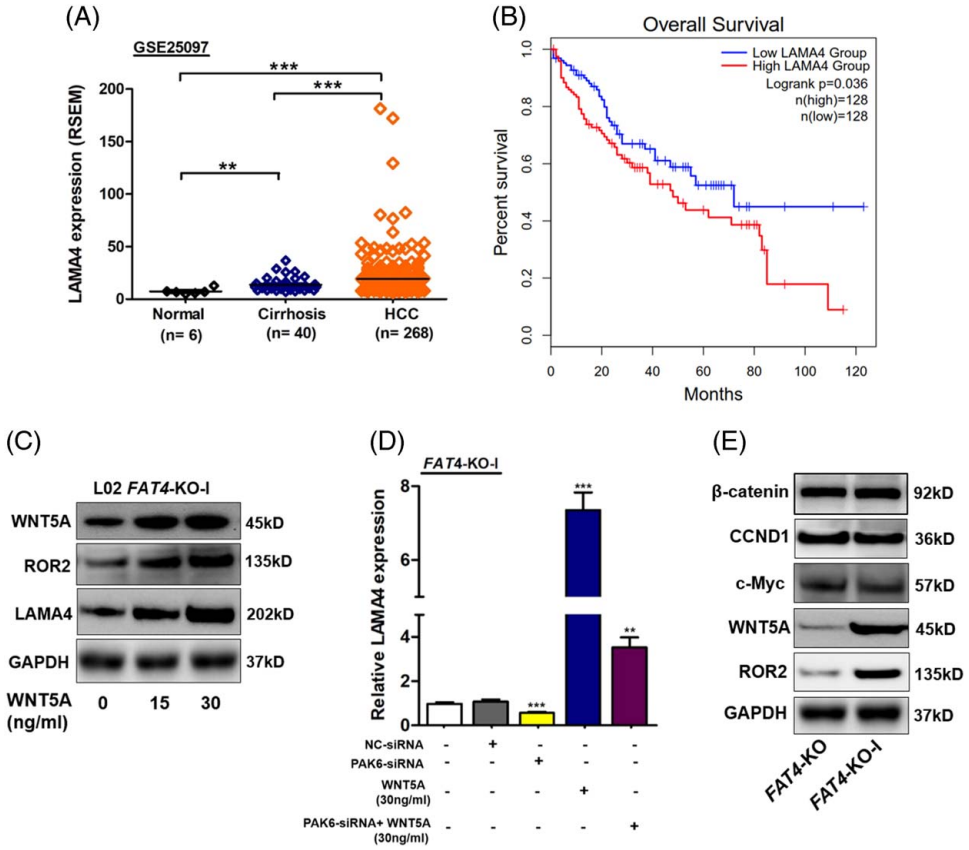

FIGURE 8 LAMA4 is a transcription target of PAK6 and WNT5A during HCC initiation and progression. (A) qPCR analysis of LAMA4 expression in normal, cirrhotic, and HCC tissues using NCBI GEO dataset (GSE25097) (B) Kaplan–Meier analysis of overall survival for 256 patients with HCC with high and low LAMA4 expression using TCGA-LIHC data. (C) Western blot analysis showed purified WNT5A treatment induced LAMA4, WNT5A, and ROR2 proteins' expression in a dose-dependent manner in amassed cells isolated from 12-day culture of *FAT4*-KO cells (L02 *FAT4*-KO-I). (D) LAMA4 mRNA expression is induced by WNT5A treatment and suppressed by knockdown of PAK6 in L02 *FAT4*-KO-I cells. (E) Western blot analysis of the expression changes in protein levels of canonical pathway proteins (β-catenin, CCND1, and c-Myc) and noncanonical pathway proteins (WNT5A and ROR2) in *FAT4*-KO cells and *FAT4*-KO-I cells $^{**}p < 0.001$, $^{*}p < 0.0001$. Abbreviations: *FAT4*, FAT atypical cadherin 4; PAK6, p21 (RAC1)-activated kinase 6; qPCR, quantitative polymerase chain reaction; TCGA-LIHC, The Cancer Genome Atlas Liver Hepatocellular Carcinoma.

out of the nucleus and aggregate in the cytoplasm for its ubiquitination-dependent degradation.[30] This was further supported by the upregulation of glycogen synthase kinase 3β and phosphor-β-catenin, and an increase in ubiquitinated proteins and ubiquitin upon PAK6 knockdown. β-catenin degradation, which resulted in the suppression of WNT/β-catenin signaling, was further evidenced by the observed downregulation of its target genes CCND1 and c-Myc, both of which are associated with tumor growth and progression.[29] Our findings showed that PAK6 has an essential role in the activation of WNT/β-catenin signaling, and silencing of PAK6 can initiate β-catenin degradation and downregulation of tumor-promoting genes such as CCND1 and c-Myc. Of note, we found phosphorylated β-catenin present in both nucleocytoplasmic cell fractions. It was suggested that the nuclear localization is possibly due to overexpression of the protein, which overloads the normal degradation mechanisms and results in nuclear translocation.[31] These data reveal the potential oncogenic role of PAK6 in cancer development; further work is required to identify whether PAK6 is involved in the initiation of HCC tumorigenesis. Besides liver fibrosis and HCC, WNT/β-catenin signaling is also a crucial pathway in stem cell maintenance and tissue homeostasis.[32,33] Thus, targeting PAK6 may offer an enormous therapeutic promise to modulate WNT/β-catenin signaling in favor of the treatment of liver fibrosis and HCC, as well as other diseases.

Increasing evidence indicates that EMT is not sufficient for tumor cell dissemination.[34] In an effort to elucidate the additional dissemination mechanisms of tumor cells, we performed RNA-seq on amassed *FAT4*-KO cells. Interestingly, in contrast to the observed upregulation of cell adhesion and ECM components such as collagens (COL9A3 and COL6A2), integrins (ITGA4 and ITGA6), and FN1 in *FAT4*-KO cells (Figure 4E-F), the expression of these adhesion and ECM components was downregulated in prolong culture of *FAT4*-KO cells (*FAT4*-KO-I) (Figure 7E and F). Alterations in ECM proteins' deposition and crosslink are vital in promoting tumor cell migration and invasion.[35] Here, we found that FAT4-KO-I cells overexpressed LAMA4, which is mainly present in tissues of mesenchymal origin.[36] LAMA4, belonging to the laminin family, is an

extracellular matrix glycoprotein. We found high LAMA4 expression is associated with poor patient survival. A high abundance of LAMA4 expression has also been reported to associate with enhanced cell migration and metastasis in HCC.[37] Activation of the noncanonical WNT5A/ROR2 signaling pathway in *FAT4*-KO-I cells had a direct effect on LAMA4 upregulation, suggesting that LAMA4 is a target of WNT5A/ROR2 signaling in HCC. To our surprise, the stimulation effect of WNT5A on LAMA4 was constrained upon PAK6 silencing. The underlying role of PAK6 in the connection between WNT/β-catenin signaling and noncanonical WNT5A signaling as tumor growth and progression is worth further investigation. Invading tumor cells attach to laminin, and the interaction increases the metastatic capacity of tumor cells.[38] Thus, the role of LAMA4 in the regulation of tumor dissemination warrants further studies, and LAMA4 overexpression might be an important marker in patients with advanced-stage HCC.

In this study, we observed the downregulation of canonical WNT/β-catenin signaling receptors and frizzled proteins (FZD8 and FZD10) in *FAT4*-KO-I cells, while the receptor ROR2 for noncanonical WNT5A signaling was upregulated. Members of the noncanonical signaling, such as WNT5A and WNT7A, have been suggested to antagonize the WNT/β-catenin signaling in a cell/receptor context-dependent manner.[39] However, we found that the noncanonical WNT5A/ROR2 signaling has no effect on the expression of β-catenin and its target genes (CCND1 and c-Myc). Thus, based on our findings, we propose that the canonical WNT/β-catenin signaling is important in early-stage tumor initiation and growth, whereas the noncanonical WNT5A/ROR2 signaling is involved in late-stage tumor migration and dissemination. The interchange of these 2 signaling pathways in hepatocarcinogenesis is dependent on the expression of its relevant signaling receptors. Our data also show upregulation of genes, such as IL-6, FGFR2, and PDGFP, which are important components of the tumor microenvironment,[40] and anti-apoptotic genes, such as MECOM and BIRC3.[41,42] Of note, upregulation of proangiogenic factor thrombospondin 1 in *FAT4*-KO-I cells has been shown to associate with tumor invasiveness and progression in HCC.[43]

In summary, the present study shows that loss of FAT4 in hepatocytes disrupts cell-cell adhesion and promotes cell transformation, which maybe a key feature of precancerous lesions and an early event in liver fibrogenesis and hepatocarcinogenesis. The interchange between canonical WNT/β-catenin signaling in the early stage of hepatocarcinogenesis and noncanonical WNT5A/ROR2 signaling during tumor progression might be valuable for the development of novel therapeutic strategies against HCC. Most importantly, our results pinpointed that PAK6 and LAMA4 maybe targets for the diagnosis and treatment of early and late HCC, respectively. This study also highlights the importance of understanding the mechanisms of HCC evolution in order to facilitate precise HCC treatment.

AUTHOR CONTRIBUTIONS

Fung-Yu Huang (Conceptualization: Lead; Investigation: Lead; Methodology: Equal; Writing original draft: Lead); Danny Ka-Ho Wong (Investigation: Equal; Methodology: Support; Writing: review and editing); Wai-Kay Seto (Investigation: Supporting; Methodology: Support; Writing: review and editing); Lung-Yi Mak (Data curation: supporting; Writing: review and editing); Tan-To Cheung (Resources: supporting; Writing: review and editing); Man-Fung Yuen (Supervision: Lead; Resources: Supporting; Writing—review & editing: Supporting).

CONFLICTS OF INTEREST

The authors declare no conflicts of interest.

ORCID

Fung-Yu Huang https://orcid.org/0000–0003–4593–1143
Danny Ka-Ho Wong https://orcid.org/0000–0001–9078–5005
Lung-Yi Mak https://orcid.org/0000–0002–2266–3935
Tan-To Cheung https://orcid.org/0000–0002–2633–5883
Sai-Sai Zhang https://orcid.org/0000–0002–3997–2144
Hau-Tak Chau https://orcid.org/0000–0003–0235–4198
Rex Wan-Hin Hui https://orcid.org/0000–0001–7447–7539
Wai-Kay Seto https://orcid.org/0000–0002–9012–313X
Man-Fung Yuen https://orcid.org/0000–0001–7985–7725

REFERENCE

1. Bataller R, Brenner DA. Liver fibrosis. J Clin Invest. 2005;115:209–18.
2. Ferlay J, Soerjomataram I, Dikshit R, Eser S, Mathers C, Rebelo M, et al. Cancer incidence and mortality worldwide: Sources, methods and major patterns in GLOBOCAN 2012. Int J Cancer. 2015;136:E359–86.
3. Kisseleva T, Brenner DA. The phenotypic fate and functional role for bone marrow-derived stem cells in liver fibrosis. J Hepatol. 2012;56:965–72.
4. Brenner DA, Kisseleva T, Scholten D, Paik YH, Iwaisako K, Inokuchi S, et al. Origin of myofibroblasts in liver fibrosis. Fibrogenesis Tissue Repair. 2012;5(Suppl 1):S17.
5. Beaussier M, Wendum D, Schiffer E, Dumont S, Rey C, Lienhart A, et al. Prominent contribution of portal mesenchymal cells to liver fibrosis in ischemic and obstructive cholestatic injuries. Lab Invest. 2007;87:292–303.
6. Wheelock MJ, Shintani Y, Maeda M, Fukumoto Y, Johnson KR. Cadherin switching. J Cell Sci. 2008;121(Pt 6):727–35.
7. Kalluri R, Weinberg RA. The basics of epithelial-mesenchymal transition. J Clin Invest. 2009;119:1420–8.
8. Komiya Y, Habas R. Wnt signal transduction pathways. Organogenesis. 2008;4:68–75.
9. Bonnet C, Brahmbhatt A, Deng SX, Zheng JJ. Wnt signaling activation: Targets and therapeutic opportunities for stem cell therapy and regenerative medicine. RSC Chem Biol. 2021;2:1144–57.
10. Bian J, Dannappel M, Wan C, Firestein R. Transcriptional Regulation of Wnt/beta-Catenin Pathway in Colorectal Cancer. Cells. 2020;9:2125.
11. Clevers H, Loh KM, Nusse R. Stem cell signaling. An integral program for tissue renewal and regeneration: Wnt signaling and stem cell control. Science. 2014;346:1248012.

12. Lam AP, Gottardi CJ. beta-catenin signaling: A novel mediator of fibrosis and potential therapeutic target. Curr Opin Rheumatol. 2011;23:562–7.
13. Sadeqzadeh E, de Bock CE, Thorne RF. Sleeping giants: Emerging roles for the fat cadherins in health and disease. Med Res Rev. 2014;34:190–221.
14. Huang FY, Wong DKH, Tsui VWM, Seto WK, Mak LY, Cheung TT, et al. Targeted genomic profiling identifies frequent deleterious mutations in FAT4 and TP53 genes in HBV-associated hepatocellular carcinoma. BMC Cancer. 2019;19:789.
15. Jones S, Zhang X, Parsons DW, Lin JCH, Leary RJ, Angenendt P, et al. Core signaling pathways in human pancreatic cancers revealed by global genomic analyses. Science. 2008;321:1801–6.
16. Crobach S, Ruano D, van Eijk R, Fleuren GJ, Minderhout I, Snowdowne R, et al. Target-enriched next-generation sequencing reveals differences between primary and secondary ovarian tumors in formalin-fixed, paraffin-embedded tissue. J Mol Diagn. 2015;17:193–200.
17. Hou L, Chen M, Zhao X, Li J, Deng S, Hu J, et al. FAT4 functions as a tumor suppressor in triple-negative breast cancer. Tumour Biol. 2016;37:16337–43.
18. Wei R, Xiao Y, Song Y, Yuan H, Luo J, Xu W. FAT4 regulates the EMT and autophagy in colorectal cancer cells in part via the PI3K-AKT signaling axis. J Exp Clin Cancer Res. 2019;38:112.
19. Malgundkar SH, Burney I, Al Moundhri M, Al Kalbani M, Lakhtakia R, Okamoto A, et al. FAT4 silencing promotes epithelial-to-mesenchymal transition and invasion via regulation of YAP and beta-catenin activity in ovarian cancer. BMC Cancer. 2020;20:374.
20. Cai J, Feng D, Hu L, Chen H, Yang G, Cai Q, et al. FAT4 functions as a tumour suppressor in gastric cancer by modulating Wnt/beta-catenin signalling. Br J Cancer. 2015;113:1720–9.
21. Huang FY, Wong DKH, Mak LY, Cheung TT, Seto WK, Yuen MF. Hepatitis B virus X protein promotes hepatocarcinogenesis via the activation of HMGA2/STC2 signaling to counteract oxidative stress-induced cell death. Carcinogenesis. 2022;43:671–81.
22. Yoshida S, Yamashita S, Niwa T, Mori A, Ito S, Ichinose M, et al. Epigenetic inactivation of FAT4 contributes to gastric field cancerization. Gastric Cancer. 2017;20:136–45.
23. Ran FA, Hsu PD, Wright J, Agarwala V, Scott DA, Zhang F. Genome engineering using the CRISPR-Cas9 system. Nat Protoc. 2013;8:2281–308.
24. Pickup MW, Mouw JK, Weaver VM. The extracellular matrix modulates the hallmarks of cancer. EMBO Rep. 2014;15:1243–53.
25. Nemeth MJ, Topol L, Anderson SM, Yang Y, Bodine DM. Wnt5a inhibits canonical Wnt signaling in hematopoietic stem cells and enhances repopulation. Proc Natl Acad Sci U S A. 2007;104:15436–41.
26. Mikels AJ, Nusse R. Purified Wnt5a protein activates or inhibits beta-catenin-TCF signaling depending on receptor context. PLoS Biol. 2006;4:e115.
27. Zeisberg M, Yang C, Martino M, Duncan MB, Rieder F, Tanjore H, et al. Fibroblasts derive from hepatocytes in liver fibrosis via epithelial to mesenchymal transition. J Biol Chem. 2007;282:23337–47.
28. Thiery JP. Epithelial-mesenchymal transitions in tumour progression. Nat Rev Cancer. 2002;2:442–54.
29. Nollet F, Berx G, van Roy F. The role of the E-cadherin/catenin adhesion complex in the development and progression of cancer. Mol Cell Biol Res Commun. 1999;2:77–85.
30. Liu C, Kato Y, Zhang Z, Do VM, Yankner BA, He X. beta-Trcp couples beta-catenin phosphorylation-degradation and regulates Xenopus axis formation. Proc Natl Acad Sci USA. 1999;96:6273–8.
31. Chung GG, Provost E, Kielhorn EP, Charette LA, Smith BL, Rimm DL. Tissue microarray analysis of beta-catenin in colorectal cancer shows nuclear phospho-beta-catenin is associated with a better prognosis. Clin Cancer Res. 2001;7:4013–20.
32. Hoffmeyer K, Raggioli A, Rudloff S, Anton R, Hierholzer A, Del Valle I, et al. Wnt/beta-catenin signaling regulates telomerase in stem cells and cancer cells. Science. 2012;336:1549–54.
33. Porfiri E, Rubinfeld B, Albert I, Hovanes K, Waterman M, Polakis P. Induction of a beta-catenin-LEF-1 complex by wnt-1 and transforming mutants of beta-catenin. Oncogene. 1997;15:2833–9.
34. Diepenbruck M, Christofori G. Epithelial-mesenchymal transition (EMT) and metastasis: Yes, no, maybe? Curr Opin Cell Biol. 2016;43:7–13.
35. Levental KR, Yu H, Kass L, Lakins JN, Egeblad M, Erler JT, et al. Matrix crosslinking forces tumor progression by enhancing integrin signaling. Cell. 2009;139:891–906.
36. Li Y, Guan B, Liu J, Zhang Z, He S, Zhan Y, et al. MicroRNA-200b is downregulated and suppresses metastasis by targeting LAMA4 in renal cell carcinoma. EBioMedicine. 2019;44:439–51.
37. Huang X, Ji G, Wu Y, Wan B, Yu L. LAMA4, highly expressed in human hepatocellular carcinoma from Chinese patients, is a novel marker of tumor invasion and metastasis. J Cancer Res Clin Oncol. 2008;134:705–14.
38. Engbring JA, Kleinman HK. The basement membrane matrix in malignancy. J Pathol. 2003;200:465–70.
39. Topol L, Jiang X, Choi H, Garrett-Beal L, Carolan PJ, Yang Y. Wnt-5a inhibits the canonical Wnt pathway by promoting GSK-3-independent beta-catenin degradation. J Cell Biol. 2003;162:899–908.
40. Fang H, Declerck YA. Targeting the tumor microenvironment: from understanding pathways to effective clinical trials. Cancer Res. 2013;73:4965–77.
41. Mendoza-Rodriguez M, Arevalo Romero H, Fuentes-Panana EM, Ayala-Sumuano JT, Meza I. IL-1beta induces up-regulation of BIRC3, a gene involved in chemoresistance to doxorubicin in breast cancer cells. Cancer Lett. 2017;390:39–44.
42. Backx E, Wauters E, Baldan J, Van Bulck M, Michiels E, Heremans Y, et al. MECOM permits pancreatic acinar cell dedifferentiation avoiding cell death under stress conditions. Cell Death Differ. 2021;28:2601–15.
43. Poon RT, Chung KK, Cheung ST, Lau CP, Tong SW, Leung KL, et al. Clinical significance of thrombospondin 1 expression in hepatocellular carcinoma. Clin Cancer Res. 2004;10(12 Pt 1):4150–7.

How to cite this article: Huang F, Wong DK, Mak L, Cheung T, Zhang S, Chau H, et al. FAT4 loss initiates hepatocarcinogenesis through the switching of canonical to noncanonical WNT signaling pathways. Hepatol Commun. 2023;7: e0338. https://doi.org/10.1097/HC9.0000000000000338